Dynamical Mechanism for Subcellular Alternans in Cardiac Myocytes

Stephen A. Gaeta, Gil Bub, Geoffrey W. Abbott, David J. Christini

Rationale: Cardiac repolarization alternans is an arrhythmogenic rhythm disturbance, manifested in individual myocytes as a beat-to-beat alternation of action potential durations and intracellular calcium transient magnitudes. Recent experimental studies have reported "subcellular alternans," in which distinct regions of an individual cell are seen to have counterphase calcium alternations, but the mechanism by which this occurs is not well understood. Although previous theoretical work has proposed a possible dynamical mechanism for subcellular alternans formation, no direct evidence for this mechanism has been reported in vitro. Rather, experimental studies have generally invoked fixed subcellular heterogeneities in calcium-cycling characteristics as the mechanism of subcellular alternans formation.

Objective: In this study, we have generalized the previously proposed dynamical mechanism to predict a simple pacing algorithm by which subcellular alternans can be induced in isolated cardiac myocytes in the presence or absence of fixed subcellular heterogeneity. We aimed to verify this hypothesis using computational modeling and to confirm it experimentally in isolated cardiac myocytes. Furthermore, we hypothesized that this dynamical mechanism may account for previous reports of subcellular alternans seen in statically paced, intact tissue.

Methods and Results: Using a physiologically realistic computational model of a cardiac myocyte, we show that our predicted pacing algorithm induces subcellular alternans in a manner consistent with theoretical predictions. We then use a combination of real-time electrophysiology and fluorescent calcium imaging to implement this protocol experimentally and show that it robustly induces subcellular alternans in isolated guinea pig ventricular myocytes. Finally, we use computational modeling to demonstrate that subcellular alternans can indeed be dynamically induced during static pacing of 1D fibers of myocytes during tissue-level spatially discordant alternans.

Conclusion: Here we provide the first direct experimental evidence that subcellular alternans can be dynamically induced in cardiac myocytes. This proposed mechanism may contribute to subcellular alternans formation in the intact heart. (*Circ Res*. 2009;105:335-342.)

Key Words: subcellular alternans ■ pattern formation ■ arrhythmia ■ calcium handling

Cardiac repolarization alternans is a disturbance in the normal rhythm of the heart that has been identified as a precursor to potentially lethal arrhythmias including ventricular tachycardia and ventricular fibrillation.[1] Alternans is seen clinically as a beat-to-beat alternation in the magnitude of the ECG T wave, which is a manifestation of underlying alternations in the durations of consecutive action potentials (APs) of individual myocytes.[2] Using calcium-sensitive indicators, these action potential duration (APD) alternations are seen to coincide with beat-to-beat alternations in the magnitude of intracellular calcium (Ca) transients, either in phase (electromechanically [EM]-concordant) or out of phase (EM-discordant), depending on the temperature and/or species.[3] Although alternans has been mechanistically linked[2,4–6] to the formation of potentially fatal reentrant arrhythmias, significant uncertainty remains regarding its mechanism and effective therapy aimed at its treatment or prevention has yet to be developed.[7] Although much recent experimental evidence has identified instabilities in intracellular Ca cycling (ie, sarcoplasmic reticulum calcium release/reuptake) as the primary cause of alternans, uncertainty remains regarding the contribution of membrane voltage (V_m) instability (caused by insufficient time for recovery of sarcolemmal ion channels between excitations) to the total instability seen in alternating cells.[1,7]

Alternans has been reported at multiple spatial scales, including spatially discordant alternans (SDA) in tissue[1] and counterphase Ca alternans in adjacent cells.[8] Most recently, several studies have reported "subcellular alternans," in which Ca transients in distinct regions of an individual myocyte alternate out of phase. Importantly, the large gradi-

Original received March 20, 2009; revision received June 11, 2009; accepted July 14, 2009.

From the Greenberg Division of Cardiology (S.A.G., G.W.A., D.J.C.) and Department of Physiology, Biophysics and Systems Biology (S.A.G., D.J.C.), Weill Cornell Medical College, New York; and Department of Physiology (G.B.), Anatomy & Genetics, University of Oxford, United Kingdom.

Correspondence to David J. Christini, Weill Cornell Medical College, 1300 York Ave, Box 161, New York, NY 10065. E-mail dchristi@med.cornell.edu

Circulation Research is available at http://circres.ahajournals.org DOI: 10.1161/CIRCRESAHA.109.197590

Non-standard Abbreviations and Acronyms	
ΔAPD	APD alternans magnitude
Δc	Ca alternans magnitude
Δc_n	Ca alternans magnitude of beat n
A_n	action potential duration of beat n
AP	action potential
APD	action potential duration
$[Ca^{2+}]_i$	cytosolic calcium concentration
c_n	peak $[Ca^{2+}]_i$ of the Ca transient of beat n
CV	conduction velocity
EM	electromechanical
g	alternans control gain
n	beat number
SDA	spatially discordant alternans
T	cycle length
V_m	membrane voltage

ents of calcium concentration formed between adjacent out-of-phase subcellular regions have been shown to predispose the cell to the formation of propagating waves of intracellular calcium release, which are thought to induce arrhythmogenic afterdepolarizations.[9–13] Subcellular alternans has been reported several times in intact tissue,[8,14] as well as in isolated cells,[10,11,15] but the cause of this phenomenon remains unclear.

Two mechanisms have been the most frequently proposed to account for the formation of subcellular alternans. The first and most prevalent attributes these subcellular differences in Ca alternans either directly or indirectly to the presence of preexisting subcellular heterogeneity in calcium-cycling components along the length of the cell.[9–11,14] In one recent example, Aistrup et al explained the subcellular alternans they observed in isolated rat hearts using a mathematical model containing significant heterogeneity in Ca-release properties in discrete regions along the length of the cell. In their model, a pacing protocol that reverses the phase of alternans (in both APD and Ca transients) can induce subcellular alternans by reversing the phase of Ca alternans in some regions earlier than others.[14]

A different hypothesis was proposed by Shiferaw and Karma, in which subcellular alternans results from a purely dynamical mechanism, in the absence of such preexisting subcellular heterogeneity.[16] They proposed a well-known dynamical pattern-forming instability (a Turing instability) as a mechanism for subcellular alternans, wherein "a fluctuation that causes the amplitude of Ca alternans to increase in a small region of the cell generates APD alternans that in turn inhibits the growth of Ca alternans far from that localized fluctuation."[16] Their theoretical analysis, however, applied to only EM-discordant myocytes, and has yet to be validated experimentally.

Here, we extend this theory to predict a novel means of dynamically inducing subcellular alternans in EM-concordant myocytes and validate this hypothesis in a computational model, as well as in isolated guinea pig ventricular myocytes. Although physiological subcellular alternans may result from a combination of both dynamical and anatomic factors, here we present the first in vitro evidence that subcellular alternans can be dynamically induced without fixed heterogeneity. Furthermore, we hypothesize that this same dynamical mechanism may contribute to subcellular alternans seen during static pacing in intact tissue.

Alternans Control

A body of literature has developed around the idea of terminating alternans for antiarrhythmic purposes.[1] The most studied approach uses nonstatic pacing in which the pacing cycle length (T) is adjusted following each AP by an amount proportional to the existing APD alternans magnitude (the difference in duration between the last 2 APs, A_n and A_{n-1}), according to the following equation:

$$\Delta T = \left(\frac{g}{2}\right)(A_n - A_{n-1}) \quad (1)$$

where g is the control gain.[17–19] Using this simple "alternans control" algorithm, the otherwise long diastolic interval following short APs is shortened and the normally short diastolic interval following long APs is lengthened. Because of a strong dependence of APD on the preceding diastolic interval (APD restitution), these continued cycle length perturbations force the APDs of an alternating cell toward an unstable period-1 rhythm. As described below, we hypothesize that alternans control dynamically induces subcellular alternans in EM-concordant cells, thereby providing a controlled means to investigate its formation in real cardiac myocytes.

Methods

An expanded Methods section is available in the Online Data Supplement at http://circres.ahajournals.org.

Briefly, computational modeling was conducted in model cells in which a single myocyte consists of a chain of 75 individual sarcomeres (each with its own calcium concentrations) coupled by calcium diffusion (as in Ref. 14, 16). The membrane voltage of all sarcomeres is explicitly synchronized. 1D fiber simulations were conducted in a 400-cell cable of such model cells, paced from the left end. This model has the distinct advantage that it is easily tuned to exhibit either positive or negative $Ca \rightarrow V_m$ coupling as well as V_m-driven, Ca-driven, or V_m and Ca-driven (hereafter "mixed instability") alternans (as described in Data Supplement). In all figures and movies, Ca alternans is quantified as $\Delta c = (-1)^n(c_n - c_{n-1})$, where c_n is the maximum $[Ca^{2+}]_i$ of each sarcomere during beat n. APD alternans is quantified as $\Delta APD = (-1)^n(A_n - A_{n-1})$, where A_n is the APD of beat n.

Experimental studies were performed in isolated left ventricular myocytes from adult Hartley guinea pigs loaded with fluo-4/acetoxymethyl ester fluorescent calcium indicator. Cells were paced at cycle lengths sufficiently fast to induce steady-state APD alternans (range, 200 to 400 ms), following which alternans control pacing (varying the cycle length in real-time using Eq. 1) and calcium imaging were initiated. All experiments were performed at room temperature.

Results

Dynamical Mechanism for Subcellular Alternans in EM-Concordant Myocytes

We hypothesized that alternans control can induce subcellular alternans in EM-concordant myocytes by a mechanism anal-

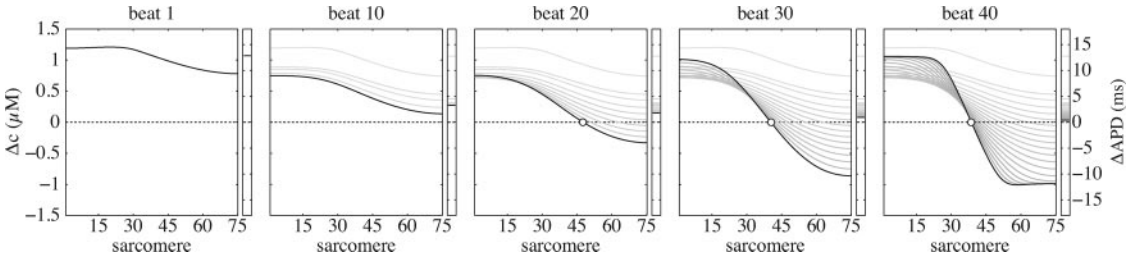

Figure 1. In the presence of fluctuations in Ca alternans (Δc) between sarcomeres, alternans control pacing induces a marked subcellular alternans pattern in the EM-concordant model cell. The graphs are snapshots from Online Video 2 showing the formation of subcellular alternans in the model myocyte when alternans control is applied. Note that in this example, a large gradient was added to initial Ca concentrations (and therefore Ca alternans magnitude [Δc]) only for the sake of clarity (as seen in the first graph). The progression to subcellular alternans is described in the text. Note that the node (the point at which Δc=0, circle) is seen to migrate to the midpoint, such that the 2 regions of opposite phase Ca alternans offset one another and a period-1 whole-cell average Ca transient (and therefore a period-1 APD) results. This simulation was performed in the mixed-instability model, T^*=300 ms (where T^* indicates target cycle length [during alternans control pacing]).

ogous to the dynamical instability previously predicted to cause subcellular alternans only in EM-discordant myocytes.[16] Alternans control is predicted to force the APDs of an alternating EM-concordant cell toward their unstable period-1 rhythm while simultaneously amplifying any small spatial fluctuations in Ca alternans magnitude into a marked subcellular alternans pattern, as follows (and seen in Figure 1).

Central to our hypothesis is the notion that the large space constant of membrane voltage relative to calcium diffusion (and the length of a single cell) allows voltage to rapidly equilibrate on the scale of an individual myocyte, whereas the Ca transients (and Ca alternans magnitudes) can vary over much smaller distances.[20] The effects of each local Ca transient on V_m (through Ca-sensitive membrane currents), however, will quickly average with the effects of all others, meaning V_m (and APD) is influenced by the whole-cell average Ca transient.

Given a perfectly homogeneous cell, the Ca transients of each sarcomere are equal to the whole-cell average Ca transient. In an EM-concordant cell, the magnitude and phase of APD alternans (itself dependent on the whole-cell average Ca transient, as above) will therefore be an accurate reflection of the local Ca alternans of each sarcomere. In such a cell, the cycle length perturbations of alternans control (which considers only ΔAPD) will appropriately control Ca alternans at all points along the length of the cell, such that all points of the cell are predicted to converge on a period-1 Ca transient rhythm (as seen in Online Video 1).

In a real cell, however, fluctuations in calcium transients (and therefore Ca alternans magnitude) exist between different subcellular regions because of, for example, the stochastic nature of calcium release, as well as any fixed subcellular heterogeneity in calcium release properties.[20] In such a cell, the alternans control perturbations, a function of only the APD, will not be appropriately sized to control Ca alternans at all points in the cell. If, for instance, some subcellular regions of the cell have Ca alternans magnitude even slightly greater than the average Ca alternans magnitude (and thus other parts have slightly less than the average), the cycle length perturbations delivered by alternans control will be too small for control of the former regions and too large for the latter.

This is seen in Figure 1 (and Online Video 2), in which a model cell (described in Methods) is paced with alternans control. Note that in this simulation, for the sake of clarity, a large, smooth gradient was added to initial Ca concentrations (and thus Ca alternans magnitude); similar results are seen with the incorporation of only small random noise (as was done in all other simulations in this study). When such a cell is far away from its period-1 rhythm, alternans control will force all regions of the cell toward their unstable period-1 Ca transient rhythm (Figure 1, first and second graphs). As control continues, however, some regions will have reached their period-1 Ca rhythm (Ca alternans magnitude=0) before the whole-cell average Ca transient is at a period-1 rhythm. Because the APD is still alternating (due to its dependence on the whole-cell average Ca transients), alternans control will continue to perturb the cycle length, reversing the phase of Ca alternans (changing the sign of Ca alternans magnitude) in those regions that had the lowest initial Ca alternans magnitude (Figure 1, third graph). For such regions of the cell, with Ca alternans now of opposite phase to that of the whole-cell average Ca alternans (and thus the APD alternans), the cycle length perturbations delivered by alternans control will now amplify these counterphase Ca alternans. The magnitude of Ca alternans in these regions will grow until the regions of opposite phase Ca alternans balance, such that the whole-cell average Ca alternans magnitude (and thus ΔAPD) will approach 0 (Figure 1, fourth graph). As this point is approached, alternans control will deliver progressively smaller perturbations to the cycle length (Eq. 1), approaching static pacing. Even with precisely static pacing, however, period-1 calcium dynamics are unstable (without such instability there would have been no alternans in the first place); Ca alternans will therefore grow in magnitude at all points along the cell, regardless of phase (Figure 1, graphs 4 and 5), forming a marked subcellular alternans.

This mechanism predicts subcellular alternans will occur in EM-concordant myocytes during alternans control but only in the presence of spatial variations in intracellular Ca concentrations (which can be satisfied by stochastic noise in initial conditions) and only if alternans is primarily driven by Ca-cycling instabilities.

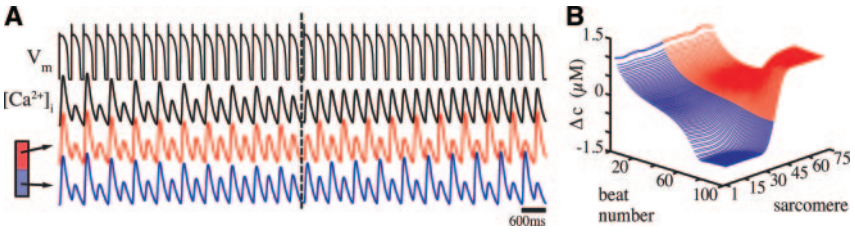

Figure 2. In the EM-concordant model, subcellular alternans occurs only when alternans control is applied. A, Alternans control is applied beginning with the fourth beat to an EM-concordant model cell, causing the APs (first black trace) and the whole-cell average Ca transients (second black trace) to converge from a period-2 rhythm (with an ΔAPD of $\approx$10 ms) to a period-1 rhythm. Concurrently, the Ca transients of the 2 halves of the cell (red and blue traces) transition from an in-phase, period-2 rhythm to a perfectly counter-phase, period-2 rhythm. Approximately 30 beats are excluded from the middle of this trace (at dashed line). B, Ca alternans magnitude (Δc) of each sarcomere is shown for the simulation in A. The simulation shown was conducted in the EM-concordant, mixed-instability model at T^*=300 ms.

Single-Cell Modeling Results

Static Pacing

When the model is tuned to exhibit EM concordance (positive Ca$\rightarrow V_m$ coupling), static pacing is unable to cause subcellular alternans at any pacing cycle length. The small degree of noise included in initial Ca concentrations quickly smoothes out through Ca diffusion between sarcomeres, which become approximately synchronized within 75 beats. To exhibit subcellular alternans during static pacing (by a Turing-type instability), the model must be tuned to EM discordance (negative Ca$\rightarrow V_m$ coupling) and Ca-driven alternans, as previously reported.[16] Interestingly, with this parameter regime, the model never exhibits APD or whole-cell Ca alternans. The Ca transients of the 2 halves of the cell are always either at a period-1 rhythm or are exactly out of phase, making the whole-cell average Ca transient a period-1 rhythm over all pacing cycle lengths (data not shown), inconsistent with most single-cell electrophysiology studies, in which APD alternans is seen with rapid pacing.

Alternans Control Induces Subcellular Alternans in an EM-Concordant Model Cell

When the model is tuned to exhibit EM concordance, although subcellular alternans is never seen with static pacing, the model does undergo a more characteristic rate-dependent alternans bifurcation into a stable period-2 APD and whole-cell concordant Ca alternans rhythm. As seen in Figure 2 and Online Video 3, alternans control forces the period-2 APD and whole-cell Ca transients toward their unstable period-1 rhythm (Figure 2A, black traces). Interestingly, this transition to a period-1 rhythm occurs simultaneously with a symmetry-breaking transition from whole-cell concordant Ca alternans to subcellular alternans, in which the 2 halves of the cell are out of phase (causing a period-1 whole-cell average Ca transient rhythm; Figure 2A and 2B). Along the length of the model cell, Ca alternans is seen to be largest at 2 terminal antinodes surrounding a single, central node with no Ca alternans. Because V_m (and thus APD) is explicitly dictated by the ionic currents averaged over the length of the cell (in this model), the effects of calcium-sensitive membrane currents in each of the 2 halves average out to produce a period-1 APD. When control is released by terminating the infinitesimally small perturbations being applied to the static pacing interval, this transition is traversed in the opposite direction, causing a smooth return to the original whole-cell concordant Ca alternans rhythm (not shown).

Subcellular alternans occurs in the EM-concordant model at all pacing cycle lengths at which alternans is seen, whenever alternans control is successful. As predicted, this effect is robust over a large range of alternans control gains above a low threshold (g>0.7 for most pacing cycle lengths) and is not seen without alternans control or in the absence of noise in initial-condition Ca concentrations. Subcellular alternans was induced in this model whenever Ca-cycling dynamics were sufficiently unstable (both the mixed instability and Ca-driven models) but, as predicted, never occurred when alternans was attributable to V_m instability. Subcellular alternans became unstable and reverted to whole-cell Ca alternans with cessation of alternans control for all cycle lengths tested.

Isolated Cell Studies

To test our hypotheses in vitro, we applied alternans control to isolated guinea pig ventricular myocytes while imaging intracellular calcium. Subcellular alternans has previously been reported in statically paced intact guinea pig heart,[8] even though guinea pig myocytes are well characterized as EM-concordant both as isolated cells[22] and in tissue.[23,24] Isolated left ventricular cells (from all myocardial regions) were paced at cycle lengths sufficiently fast to induce steady-state alternans (range 200 to 400 ms), after which alternans control was initiated. A total of 51 trials were conducted in 16 different cells (an average of 4 trials were performed in each cell). All recordings showed EM concordance throughout. Alternans control successfully suppressed alternans (in both APD and whole-cell average Ca transient magnitude) in 45 of the 49 trials in which it was applied, and 42 of those 45 successful trials showed subcellular Ca alternans (as in Figure 3A through 3C; Online Videos 5 and 6). Subcellular alternans was never seen without control, and none of the trials in which control failed showed subcellular alternans. This effect was seen at all cycle lengths tested (at which alternans occurred), independent of alternans control gain, and was robust to changes in patch-clamp configuration (perforated versus ruptured patch) and dye affinity (Fluo-4 versus Fluo-4 FF).

In 13 of 17 trials in which alternans control was released (static pacing resumed) during imaging, subcellular alternans

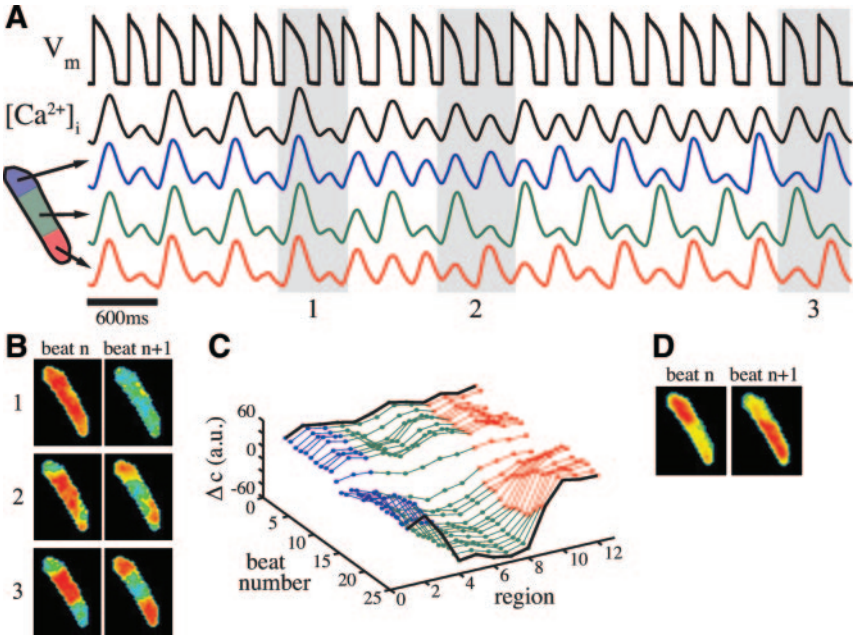

Figure 3. Alternans control induces subcellular alternans in an isolated ventricular myocyte. A, Alternans control causes a steady-state, period-2 APD (first black trace) and whole-cell Ca alternans (second black trace) to transition to a period-1 rhythm. Concurrently, the spatially homogenous Ca alternans transitions to a 2-node subcellular alternans. Blue, green, and red traces are the average fluorescence from the 3 regions diagrammed. B, Recorded fluorescence frames at the time of maximum calcium concentration in 2 successive beats during initial control (1), during the transition (2), and at nearly period-1 control (3); beat pairs are marked by gray shaded regions in A. C, Ca alternans magnitude along the length of the cell is plotted for the experiment shown in A. For this graph, fluorescence data are binned into 12 adjacent regions perpendicular to the length of the cell and the average Ca alternans magnitude (Δc) is plotted for each region for the 25 beats shown (arbitrary fluorescence units), with colors corresponding to the regions diagrammed in A. Fluorescence data from the extreme ends of the cell are excluded because of motion artifact. D, This same cell in a different trial (at the same pacing cycle length) exhibited a different pattern of subcellular alternans (1 node) when alternans control was applied. Experiments shown are from a cell paced at T^*=300 ms.

transitioned back to whole-cell concordant alternans (as in Figure 4; Online Videos 5 and 6). In the 4 trials in which the subcellular alternans persisted after control was released, the APDs diverged to stable alternans after imaging had ended, implying that a longer imaging period would have captured a return to whole-cell concordant Ca alternans as well.

Six of the 16 cells tested showed more than 1 node (and more than 2 antinodes) of Ca alternans during alternans control in one or more trials, in patterns similar to those seen in the mathematical model (as in Figure 3A through 3C, Online Figure I, and Online Video 6). The majority of cells showed a similar pattern and number of nodes in each trial, but 5 of the 16 cells exhibited different numbers of nodes in different trials at the same cycle length (as seen in Figure 3B and 3D).

One-Dimensional Fiber Simulations

We further hypothesized that previous reports of subcellular alternans in statically paced, intact tissue[8,14] may also be accounted for by our proposed dynamical mechanism. In particular, the cycle length perturbations induced by the alternans control protocol are directly analogous to the local activation times of cells away from the pacing site in whole heart given sufficiently steep conduction velocity (CV) restitution.[21] We therefore predicted that given sufficiently steep CV restitution, subcellular alternans can be induced by the same dynamical mechanism in EM concordant tissue during static pacing.

To test this hypothesis, we implemented a cable of 400 model cells, each one itself a cable of 75 sarcomeres. The cells were tuned to be EM-concordant, with calcium-driven alternans (as described in the Online Methods) and contained no fixed heterogeneity in Ca-release properties. The left-most 5 cells of the cable were statically paced for 300 beats at a slow cycle length (T=400 ms, at which there is no alternans at any spatial scale) and then for an additional 200 beats at a faster cycle length (either 330 or 320 ms). When the pacing cycle length was decreased to T=330 ms, CV-restitution was not steep enough to induce tissue-level SDA. In this case, alternans is seen in the Ca transients of every sarcomere, as well as the APD of every cell, but subcellular alternans is not observed (Figure 5A). In contrast, when the pacing cycle length is decreased to 320 ms, tissue-level SDA arises in both the APD and the whole-cell average calcium transient (Figure 5B, top and middle). Additionally, over the course of the 200 beats at this faster cycle length, a prominent subcellular alternans transiently develops in the cells near the node of tissue-level SDA (Figure 5B, bottom). Figure 5C shows a pseudo–line scan image of a single cell near the node of SDA (the cell with the most significant subcellular alternans). The patterns of subcellular alternans formed were similar to those seen in previous experiments in intact rat heart (Ref. 8, 14), with nodes (dashed lines) migrating along the length of the cell as the simulation progressed until the entire cell has reversed phase of Ca alternans. Note that in this model the membrane voltage is explicitly synchronized for all sarco-

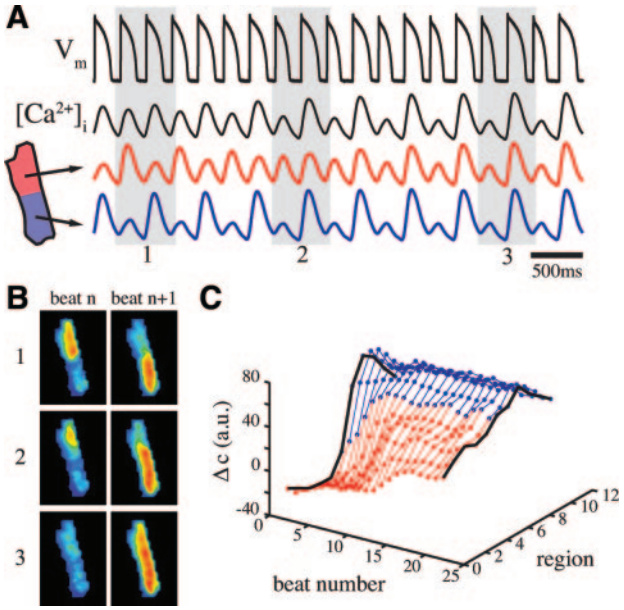

Figure 4. During static pacing, subcellular alternans is unstable and transitions back to whole-cell concordant Ca alternans. Alternans control was used to force a cell to near its period-1 APD rhythm (thereby inducing a 1-node subcellular alternans), at which point static pacing was resumed. A, V_m (first black trace), whole-cell average calcium fluorescence (second black trace), and average fluorescence from the 2 halves of the cell (red and blue traces) are shown following resumption of static pacing (following beat 1). The subcellular alternans is seen to transition back to a whole-cell concordant Ca alternans rhythm, concurrent with a transition from a nearly period-1 APD rhythm to a clear APD alternans. B, Recorded fluorescence frames at the time of maximum calcium concentration in 2 successive beats immediately after control is released (1), several beats later (2), and after return to whole-cell concordant APD and Ca alternans (3). C, Ca alternans magnitude (Δc) along the length of the cell is plotted for the experiment shown in A (as described in Figure 1, with 10 binned regions). Experiment shown is from a cell paced at T^*=250 ms.

meres in each myocyte. Subcellular pattern formation in these simulations reflects a purely dynamical phenomenon.

Discussion

Subcellular Ca alternans has been reported multiple times in the intact heart as well as in isolated cardiac myocytes, but the mechanism for this striking phenomenon remains unclear. Although previous studies have invoked subcellular heterogeneities in Ca-cycling characteristics to explain the occurrence of subcellular alternans, we believe that the rich cardiac myocyte dynamics (which are known to contribute to alternans at the cellular and tissue level) cannot be discounted. An elegant theoretical study proposed a dynamical mechanism for subcellular alternans,[16] but it was believed relevant to only a subset of cardiac myocytes (EM-discordant cells) and has never been verified experimentally. We have shown that this same dynamical mechanism is predicted to cause subcellular alternans in the remaining subset of myocytes (EM-concordant cells) during alternans control pacing and have verified this prediction using computational modeling and in vitro electrophysiology. Importantly, this mechanism can induce subcellular alternans in the absence of subcellular heterogeneity in Ca-cycling characteristics. Although this mechanism can also induce subcellular alternans in the presence of such heterogeneity, the patterns seen experimentally do not suggest that such heterogeneity plays a major role (Online Results and Online Figure I). Importantly, alternans control represents a controlled means of inducing this phenomenon in real cells, allowing in vitro confirmation for the first time.

Alternans Control Induces Subcellular Alternans in EM-Concordant Myocytes

When alternans control pacing was applied to an EM-concordant mathematical model, subcellular alternans was induced in a robust manner. Notably, subcellular alternans was induced in this manner without the need for fixed heterogeneity, thus predicting that a purely dynamical mechanism can induce subcellular alternans. Our in vitro studies similarly demonstrated that alternans control robustly induces subcellular alternans in (EM-concordant) isolated guinea pig ventricular myocytes. We believe that although there is undoubtedly fixed subcellular heterogeneity in real myocytes, our results support a primarily dynamical induction of subcellular alternans in our experiments and do not suggest the presence of heterogeneity of the type previously proposed to account for subcellular alternans formation.

Several experimental observations support these conclusions. (1) A change from static pacing to alternans control was sufficient to robustly induce a smooth transition to subcellular alternans. This agrees with our theoretical and mathematical modeling work, in which this pacing algorithm can induce subcellular alternans in cells by a purely dynamical mechanism. (2) Release of alternans control (resumption of static pacing) during subcellular alternans caused this rhythm to lose stability and return to a period-2 APD and whole-cell concordant Ca alternans rhythm. It is important to note that successful alternans control (as was achieved before release in Figure 4) forces a cell toward its period-1 rhythm with progressively smaller perturbations to the cycle length, culminating in very small changes to the pacing interval around the target cycle length (nearly static pacing). As such, the transition from alternans control to static pacing is a smooth transition. (3) The nodes of subcellular alternans were distributed approximately symmetrically about the midline, as has been reported in several other studies.[8,10,11,15] In contrast, our mathematical modeling results indicate that in the presence of the large, fixed gradients of calcium-cycling components previously proposed to cause subcellular alternans (Online Figure I, B), the pattern of subcellular alternans would be strongly dependent on the distribution of this underlying heterogeneity. We are unaware of any previous work that suggests the presence of the symmetrical gradients of subcellular heterogeneity that would be required for the symmetrical pattern of subcellular alternans seen in our experimental studies (and those of others) to be caused by underlying heterogeneity alone. (4) The patterns of subcellular alternans were seen to vary in different trials of the same cell at the same cycle length (5/16 cells; as in Figure 3B and 3D). This is consistent with the dynamical model of Online Figure I, A, but inconsistent with the predictions of the model when large, fixed gradients of calcium-cycling components

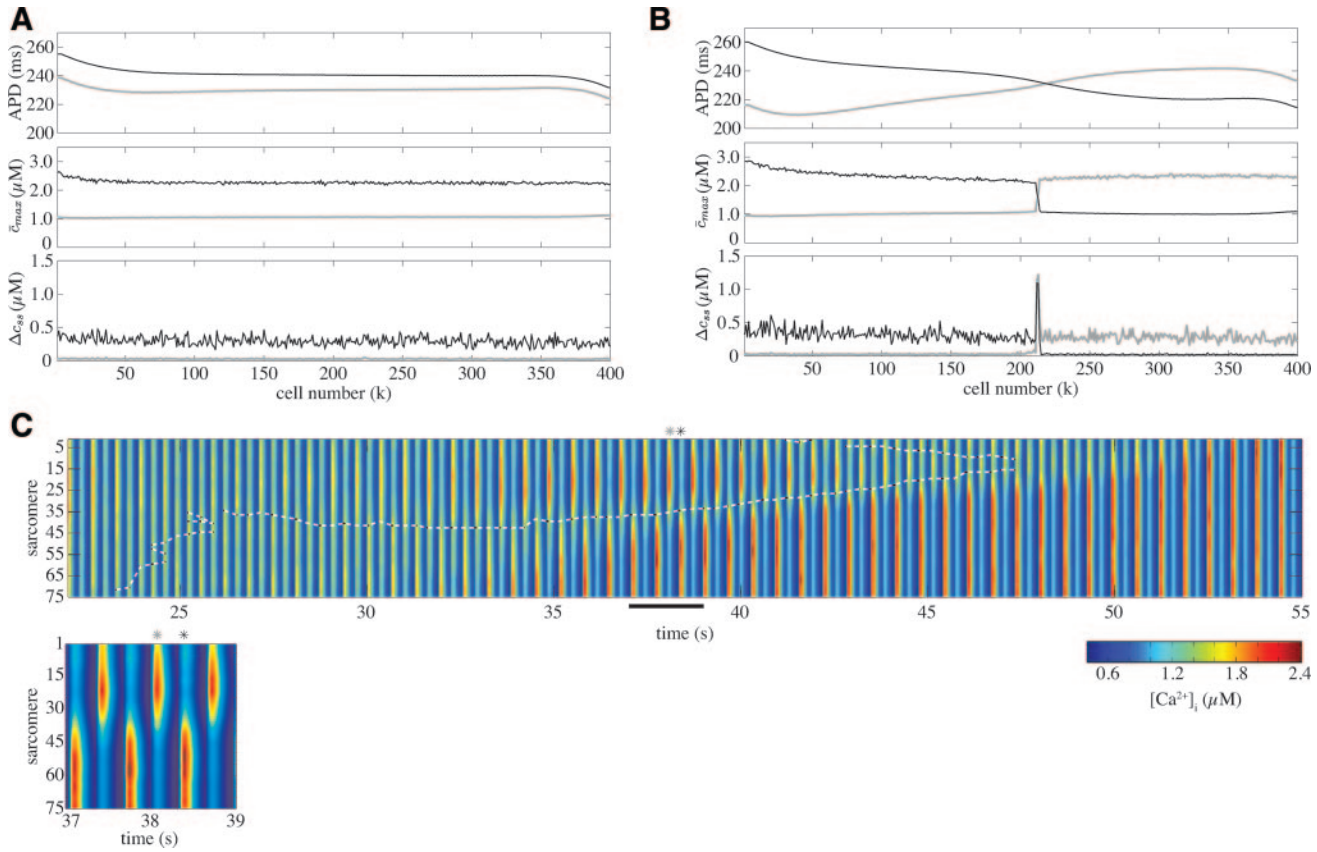

Figure 5. Subcellular alternans is dynamically induced during static pacing of a simulated 1D fiber of EM-concordant myocytes when tissue-level SDA forms. A 1D fiber of model myocytes was stimulated (from the left) for 300 beats at pacing cycle length $T=400$ ms and then stepped down to 330 ms (A) and 320 ms (B) for an additional 200 beats. Results from beats n=419 (gray) and 420 (black) are shown. In A, the lack of SDA in APD (top) and in whole-cell average Ca transients (middle) is accompanied by no subcellular alternans (bottom). For each cell, $\bar{c}_{max}$ is the peak concentration of the whole-cell average Ca transient and Δc_{ss} is the difference in peak Ca concentration between the largest and smallest subcellular Ca transients of each cell during a given beat. Note that the baseline level of Δc_{ss} is nonzero because of noise added to the calcium concentration of each sarcomere before every stimulus. In B, tissue-level SDA is seen in both the APD (top) and whole-cell average Ca transients (middle). As the node of SDA migrates from the right of the cable to its steady-state location, cells adjacent to the node undergo a transient rise in subcellular alternans (seen here in cell 213). C, A pseudo–line scan plot of $[Ca^{2+}]_i$ for cell 213 in B showing the calcium transients of every sarcomere and the movement of the period-1 node (dashed line) from 22.5 to 55 seconds after the cycle length was decreased. Inset is a magnification of time 37 to 39 seconds, during which beats 419 (gray star) and 420 (black star) occurred.

were included (Online Figure I, B). Notably, with only a small degree of stochastic fixed heterogeneity in calcium-cycling components, the model was seen to exhibit different patterns in different trials with nodes symmetrically distributed about the midline, consistent with our experimental results. Future studies using confocal imaging will be needed to precisely determine 3D cellular morphology and the location of nodal lines during subcellular alternans.

Notably, the occurrence of subcellular alternans during alternans control is only predicted when Ca-cycling instability is greater than instability attributable to membrane voltage dynamics (if this were not the case, all Ca transients would alternate secondary to APD alternans and would thus be synchronized). The occurrence of subcellular alternans in our guinea pig myocytes therefore supports the findings of several previous studies indicating that alternans is primarily attributable to Ca-cycling dynamics.[1] Testing for subcellular alternans during alternans control pacing may represent a useful tool for determining the primary source of instability in other cell types/species, as well as at different pacing cycle lengths.

Subcellular Alternans May Be Dynamically Induced in Intact Tissue During Static Pacing

The dynamical induction of subcellular alternans in EM-concordant myocytes may also occur physiologically, and may contribute to rate-dependent subcellular alternans seen in statically paced intact tissue.[8,14] In tissue, at sufficiently fast pacing rates, the effect of steep CV restitution produces an effect similar to alternans control in the local activation times of cells distant from the pacing site. Specifically, if APD alternans occurs at the pacing site during static pacing, CV-restitution dictates that "long" APs will propagate away faster than "short" APs. Cells away from the pacing site will thus experience effectively nonstatic pacing, with the excitations following their "long" APDs arriving late (because they are carried by a more slowly traveling, "short" AP) and those following their "short" APDs arriving early (because they are carried by a faster, "long" AP). The further away from the pacing site, the greater the effect of propagation velocity on cycle length, and the stronger is this alternans control-like effect. Indeed, these cycle length alternations can be strong

enough to entirely eliminate APD alternans (forming a period-1 node) and, even further away, reverse the phase of APD alternans relative to that at the pacing site (forming tissue-level SDA). Notably, such cycle length alternations were observed concomitant with the subcellular alternans recently observed during static pacing of rat heart.[14]

Indeed, we found that when tissue-level SDA is induced by static pacing in a simulated 1D fiber of EM-concordant myocytes, subcellular alternans is dynamically induced in those cells adjacent to the tissue-level node (where cycle length alternations are the most pronounced). Although there are clearly many dynamical and anatomic differences between isolated cells and the intact heart, we believe that the proposed dynamical mechanism may contribute to the formation of physiological subcellular alternans.

It is important to note that although subcellular alternans can be induced dynamically in isolated cells, the physiological formation of subcellular alternans is likely governed by a rich interplay of dynamical as well as anatomic factors. Still, we believe that our identification of a robust, dynamical mechanism by which subcellular alternans can be induced in isolated cardiac myocytes not only provides novel insights into the mechanism of this phenomenon in the real heart but also will facilitate future studies into the formation and consequences of subcellular alternans and biological pattern formation.

Acknowledgments

We gratefully acknowledge Dr Andrew Zygmunt and Dr Lai-Hua Xie for valuable technical assistance and Dr Yohannes Shiferaw for providing model code.

Sources of Funding

This work was supported by NIH Medical Scientist Training Program grant GM07739 (to S.A.G.), NIH grant R01RR020115 (to D.J.C.), and the Kenny Gordon Foundation.

Disclosures

None.

References

1. Weiss JN, Karma A, Shiferaw Y, Chen PS, Garfinkel A, Qu Z. From pulsus to pulseless: the saga of cardiac alternans. *Circ Res*. 2006;98:1244–1253.
2. Pastore JM, Girouard SD, Laurita KR, Akar FG, Rosenbaum DS. Mechanism linking T-wave alternans to the genesis of cardiac fibrillation. *Circulation*. 1999;99:1385–1394.
3. Euler DE. Cardiac alternans: mechanisms and pathophysiological significance. *Cardiovasc Res*. 1999;42:583–590.
4. Chinushi M, Kozhevnikov D, Caref EB, Restivo M, El-Sherif N. Mechanism of discordant T wave alternans in the in vivo heart. *J Cardiovasc Electrophysiol*. 2003;14:632–638.
5. Chinushi M, Restivo M, Caref EB, El-Sherif N. Electrophysiological basis of arrhythmogenicity of QT/T alternans in the long-QT syndrome: tridimensional analysis of the kinetics of cardiac repolarization. *Circ Res*. 1998;83:614–628.
6. Shimizu W, Antzelevitch C. Cellular and ionic basis for T-wave alternans under long-QT conditions. *Circulation*. 1999;99:1499–1507.
7. Jordan PN, Christini DJ. Characterizing the contribution of voltage- and calcium-dependent coupling to action potential stability: implications for repolarization alternans. *Am J Physiol Heart Circ Physiol*. 2007;293:H2109–H2118.
8. Aistrup GL, Kelly JE, Kapur S, Kowalczyk M, Sysman-Wolpin I, Kadish AH, Wasserstrom JA. Pacing-induced heterogeneities in intracellular Ca2+ signaling, cardiac alternans, and ventricular arrhythmias in intact rat heart. *Circ Res*. 2006;99:e65–e73.
9. Blatter L. Local calcium gradients during excitation-contraction coupling and alternans in atrial myocytes. *J Physiol*. 2003;546:19–31.
10. Díaz ME, Eisner DA, O'Neill SC. Depressed ryanodine receptor activity increases variability and duration of the systolic Ca2+ transient in rat ventricular myocytes. *Circ Res*. 2002;91:585–593.
11. Kockskämper J, Blatter LA. Subcellular Ca2+ alternans represents a novel mechanism for the generation of arrhythmogenic Ca2+ waves in cat atrial myocytes. *J Physiol (Lond)*. 2002;545(pt 1):65–79.
12. De Ferrari GM, Viola MC, D'Amato E, Antolini R, Forti S. Distinct patterns of calcium transients during early and delayed afterdepolarizations induced by isoproterenol in ventricular myocytes. *Circulation*. 1995;91:2510–2515.
13. Miura M, Ishide N, Oda H, Sakurai M, Shinozaki T, Takishima T. Spatial features of calcium transients during early and delayed afterdepolarizations. *Am J Physiol*. 1993;265(2 pt 2):H439–H444.
14. Aistrup GL, Shiferaw Y, Kapur S, Kadish AH, Wasserstrom JA. Mechanisms underlying the formation and dynamics of subcellular calcium alternans in the intact rat heart. *Circ Res.* 2009;104:639–649.
15. Cordeiro JM, Malone JE, Di Diego JM, Scornik FS, Aistrup GL, Antzelevitch C, Wasserstrom JA. Cellular and subcellular alternans in the canine left ventricle. *Am J Physiol Heart Circ Physiol*. 2007;293:H3506–H3516.
16. Shiferaw Y, Karma A. Turing instability mediated by voltage and calcium diffusion in paced cardiac cells. *Proc Natl Acad Sci U S A*. 2006;103:5670–5675.
17. Hall GM, Gauthier DJ. Experimental control of cardiac muscle alternans. *Phys Rev Lett*. 2002;88:198102.
18. Hall K, Christini DJ. Restricted feedback control of one-dimensional maps. *Phys Rev E Stat Nonlin Soft Matter Phys.* 2001;63(4 pt 2):046204.
19. Christini DJ, Riccio ML, Culianu CA, Fox JJ, Karma A, Gilmour RF. Control of electrical alternans in canine cardiac purkinje fibers. *Phys Rev Lett*. 2006;96:104101.
20. Cannell MB, Cheng H, Lederer WJ. Spatial non-uniformities in [Ca2+]i during excitation-contraction coupling in cardiac myocytes. *Biophys J*. 1994;67:1942–1956.
21. Watanabe MA, Fenton FH, Evans SJ, Hastings HM, Karma A. Mechanisms for discordant alternans. *J Cardiovasc Electrophysiol*. 2001;12:196–206.
22. Wan X, Laurita KR, Pruvot EJ, Rosenbaum DS. Molecular correlates of repolarization alternans in cardiac myocytes. *J Mol Cell Cardiol*. 2005;39:419–428.
23. Choi BR, Salama G. Simultaneous maps of optical action potentials and calcium transients in guinea-pig hearts: mechanisms underlying concordant alternans. *J Physiol.* 2000;529(pt 1):171–188.
24. Pruvot EJ, Katra RP, Rosenbaum DS, Laurita KR. Role of calcium cycling versus restitution in the mechanism of repolarization alternans. *Circ Res.* 2004;94:1083–1090.